ARTICLE

Zeb1 represses TCR signaling, promotes the proliferation of T cell progenitors and is essential for NK1.1$^+$ T cell development

Jiang Zhang[1,2], Mélanie Wencker[1], Quentin Marliac[1], Aurore Berton[1], Uzma Hasan[1], Raphaël Schneider[3], Daphné Laubreton[1], Dylan E. Cherrier[1], Anne-Laure Mathieu[1], Amaury Rey[1], Wenzheng Jiang[2], Julie Caramel[4], Laurent Genestier[4], Antoine Marçais[1], Jacqueline Marvel[1], Yad Ghavi-Helm[3] and Thierry Walzer[1]

T cell development proceeds under the influence of a network of transcription factors (TFs). The precise role of Zeb1, a member of this network, remains unclear. Here, we report that Zeb1 expression is induced early during T cell development in CD4$^-$CD8$^-$ double-negative (DN) stage 2 (DN2). Zeb1 expression was further increased in the CD4$^+$CD8$^+$ double-positive (DP) stage before decreasing in more mature T cell subsets. We performed an exhaustive characterization of T cells in *Cellophane* mice that bear *Zeb1* hypomorphic mutations. The Zeb1 mutation profoundly affected all thymic subsets, especially DN2 and DP cells. Zeb1 promoted the survival and proliferation of both cell populations in a cell-intrinsic manner. In the periphery of *Cellophane* mice, the number of conventional T cells was near normal, but invariant NKT cells, NK1.1$^+$ γδ T cells and Ly49$^+$ CD8 T cells were virtually absent. This suggested that Zeb1 regulates the development of unconventional T cell types from DP progenitors. A transcriptomic analysis of WT and *Cellophane* DP cells revealed that Zeb1 regulated the expression of multiple genes involved in the cell cycle and TCR signaling, which possibly occurred in cooperation with Tcf1 and Heb. Indeed, *Cellophane* DP cells displayed stronger signaling than WT DP cells upon TCR engagement in terms of the calcium response, phosphorylation events, and expression of early genes. Thus, Zeb1 is a key regulator of the cell cycle and TCR signaling during thymic T cell development. We propose that thymocyte selection is perturbed in *Zeb1*-mutated mice in a way that does not allow the survival of unconventional T cell subsets.

Keywords: T cell selection; TCR signaling; Zeb1; transcription; development

Cellular & Molecular Immunology (2021) 18:2140–2152; https://doi.org/10.1038/s41423-020-0459-y

INTRODUCTION

T cell development occurs in the thymus and begins in immature thymocytes that are double negative (DN) for CD4 and CD8 expression. The DN population can be subdivided into four subsets, DN1–DN4, depending on the expression of the cell surface molecules CD44 and CD25 (for a review, see[1]). DN1 cells (CD44$^+$CD25$^-$) are the most immature progenitors and retain the ability to differentiate into non-T cell lineages. In DN2 cells (CD44$^+$CD25$^+$), the expression of RAG1/2 is induced, which promotes the rearrangement of gene segments encoding the TCR-β, TCR-γ, and TCR-δ subunits. In DN3 cells (CD44$^-$CD25$^+$), the T cell antigen receptor (TCR) β-chain associates with the pre-TCR α-chain and CD3 subunits to form the pre-TCR complex; the pre-TCR complex allows β-selection to occur. During β-selection, DN3 cells with productive TCRβ rearrangements receive survival and proliferative signals and mature into the DN4 (CD44$^-$CD25$^-$) stage. DN4 thymocytes then develop into CD4$^+$CD8$^+$ double-positive (DP) cells.[2]

At the DP stage, a series of events takes place that determines the fate of developing T cells, including rearrangement of the TCR alpha locus, association of the αβ T cell receptor, and subsequent thymic selection. In general, high-affinity interactions between the αβTCR and self-peptide-MHC complexes presented by different thymic cells lead to negative selection and elimination of self-reactive thymocytes, while low-affinity interactions result in positive selection and development of CD4 or CD8 single-positive (SP) T cells.[3–5] Despite this general rule, regulatory T cells and invariant NKT cells (iNKT) receive stronger TCR signals than conventional T cells during their development[6] as a result of selection by agonist self-antigens. iNKT cells are a subset of innate-like T cells with a single invariant TCRα chain (Vα14-Jα18 in mice) and a limited repertoire of TCRβ chains (Vβ8.2, Vβ7, or Vβ2) that recognize glycolipid antigens bound to CD1d, a nonpolymorphic MHC molecule.[7] iNKT cell development includes discrete stages (stages 0–3) that can be discriminated according to CD44 and NK1.1 expression.[8] Three functionally distinct iNKT cell subsets have also been identified: iNKT1 cells, which express T-bet and mainly secrete IFN-γ; iNKT2 cells, which express Gata3 and Plzf and secrete IL-4 and IL-13; and iNKT17 cells, which express Rorγt and secrete IL-17. The TCR signal strength during selection governs the development of iNKT cell subsets, with strong signals promoting iNKT2 and iNKT17 development.[9,10] A large number of molecules

[1]CIRI, Centre International de Recherche en Infectiologie, Univ Lyon, Inserm, U1111, Université Claude Bernard Lyon 1, CNRS, UMR5308, ENS de Lyon, F-69007 Lyon, France; [2]Shanghai Key Laboratory of Regulatory Biology, School of Life Sciences, East China Normal University, Shanghai, China; [3]Institut de Génomique Fonctionnelle de Lyon, CNRS UMR 5242, Ecole Normale Supérieure de Lyon, Université Claude Bernard Lyon 1, 46 allée d'Italie, F-69364 Lyon, France and [4]CRCL, Centre de Recherche sur le Cancer de Lyon, INSERM U1052—CNRS UMR5286, Centre Léon Bérard, Université Claude Bernard Lyon 1, Lyon, France
Correspondence: Thierry Walzer (thierry.walzer@inserm.fr)

Received: 5 November 2019 Revised: 22 April 2020 Accepted: 23 April 2020
Published online: 12 May 2020

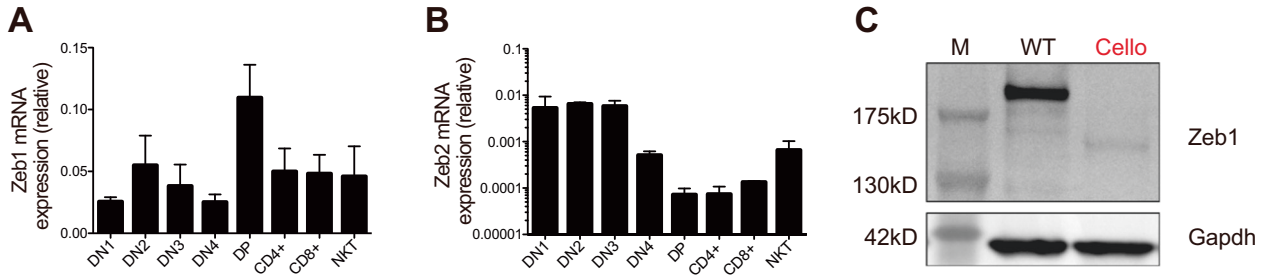

Fig. 1 Zeb1 expression in WT and *Cellophane* thymocytes. **a**, **b** RT-PCR analysis of RNA from sorted thymocyte subsets isolated from C57BL/6 mice, as indicated. The results are presented relative to the expression of the control gene *Gapdh*. **c** WB analysis of Zeb1 expression in total thymocytes from WT and *Cellophane* mice, as indicated. Data are representative of three independent experiments with three to six mice (**a**, **b**) or three independent experiments with three mice (**c**)

regulate the strength of TCR-derived signaling. TCR signaling strength can also be modulated at the transcriptional level by transcription factors (TFs) such as Sox4[11] or at the posttranscriptional level by miR-181.[12,13] The loss of either Sox4 or miR-181 blocks iNKT cell development. Mechanistically, miR-181a regulates the expression of multiple phosphatases and other proteins to boost TCR signaling as well as cell metabolism.[12,13] Interestingly, mice expressing a hypomorphic form of Zap70, a major TCR-proximal kinase, also show impaired developmental maturation of γδ T cells, suggesting that innate-like T cell subsets are particularly dependent on the tight regulation of the strength of TCR signaling for their development.[14]

A dense network of TFs has been shown to regulate T cell development.[15] Early commitment is dependent on Notch signaling,[16] which induces the expression of many TFs and maintains their expression throughout T cell development. Among these TFs, the E-protein family factors E2a, Tcf1 (encoded by *Tcf7*) and Heb (encoded by *Tcf12*)[17] induce the expression of TCR components and balance the survival and proliferation of thymocytes.[18] Many other TFs, such as Gata3, Myb, Runx1, and Bcl11b, also cooperate with E proteins at different developmental stages and further establish T cell identity.[15,18]

The Zeb family of TFs consists of Zeb1 and Zeb2, which are best known for their role in epithelial-to-mesenchymal transition (EMT). EMT programs operate at different stages of embryonic development and are downstream of Wnt, TGF-β, Bmp, Notch, and other signaling pathways.[19] *Zeb1*$^{-/-}$ mice exhibit multiple developmental defects and die at birth.[20] Under pathological conditions, activation of EMT programs contributes to fibrosis and cancer metastasis.[21] Zeb1 and Zeb2 are highly homologous and are characterized by two clusters of zinc finger domains at the protein extremities. They also contain a homeodomain and a Smad-binding domain and can interact with many other TFs.[22] Zeb1 and Zeb2 are also expressed in a tightly regulated manner in the immune system and regulate cell differentiation.[23] We and others have previously shown that Zeb2 regulates terminal NK cell[24] and effector CD8 T cell differentiation.[25,26] Mutated mice expressing a truncated form of Zeb1 without the C-terminal zinc finger clusters at C727 have a small and hypocellular thymus, which is the result of a reduction in early T cell precursors.[27] In *Cellophane* mutant mice, a T → A mutation in the seventh exon of *Zeb1* replaces the tyrosine at position 902 with a premature stop codon.[28] The resulting mRNA encodes a truncated protein lacking the C-terminal zinc finger domain, which is predicted to be hypomorphic. *Cellophane* homozygous mice have small, hypocellular thymi with decreased DP thymocytes. However, the mechanism of Zeb1 action during T cell development and its role in the maturation of T cell subsets remain unclear. Here, we show that *Cellophane* homozygous mice lack several peripheral T cell subsets, including iNKT cells, NK1.1^{+} γδ T cells, and Ly49-expressing CD8 T cells. This specific defect involving innate-like T cells is caused by the cell-intrinsic role of Zeb1 in T cell development. We show that Zeb1 expression is maximal in the DN2 and DP stages of T cell development. Furthermore, Zeb1 regulates the transition to the SP stage by promoting cell proliferation and survival and repressing the expression of various molecules that modulate the strength of TCR signaling. Therefore, we propose that Zeb1 is a key regulator of thymocyte selection that is essential for the development and survival of innate-like T cell subsets undergoing agonist-type selection.

RESULTS

Zeb1 is highly expressed in the DN2 and DP stages of T cell development

To study the role of Zeb1 in T cell development, we sorted thymocyte subsets and measured Zeb1 transcript levels by semiquantitative (Q) RT-PCR (reverse transcription-polymerase chain reaction). As shown in Fig. 1a, Zeb1 transcript levels were low in DN1, began to increase in the DN2 stage and were maximal in DP thymocytes. Zeb1 expression then decreased as T cells underwent selection and matured into either conventional T cells or iNKT cells. Interestingly, the expression of Zeb2 was somewhat similar to that of Zeb1; high expression of Zeb2 was observed in early thymic progenitors (DN1–DN4), and the lowest expression of Zeb2 was observed in DP cells (Fig. 1b). This pattern of expression was corroborated by data from the ImmGen consortium[29] (Fig. S1A). Thus, as was observed in memory T cells,[30] Zeb1 and Zeb2 show similar patterns of expression in thymocytes. We used the ImmGen web browser to search for coregulated genes across different immune subsets. The E-protein Heb (encoded by *Tcf12*) was among the top 3 genes found to be coregulated with Zeb1 (Fig. S1B).[29] Heb is well known for its important roles throughout T cell development,[31] especially in the DP stage,[32] which further indicates that Zeb1 is a potential regulator of the DP developmental stage. We also analyzed the expression of Zeb1 protein in total thymocytes (80% of which consist of DPs). Zeb1 was strongly expressed in WT thymocytes but not in *Cellophane* thymocytes. Mutant mice expressed only reduced quantities of a truncated form of Zeb1 (Fig. 1c).

Impaired development of both conventional and unconventional T cells in *Cellophane* mice

To define the impact of the *Cellophane* mutation on T cell development, we analyzed the T cell composition in the thymus, spleen, and lymph nodes (LNs) of *Cellophane* mice. The T cell numbers in the spleen and liver were normal, while the number of lymphocytes was reduced in LNs (Fig. 2a). As shown by previous findings,[28] we also observed a strong decrease in the cell numbers in the thymus in *Zeb1*-mutated mice (Fig. 2a). This decrease in the cell number affected all subsets defined by CD4, CD8, CD44, and CD25 expression (Fig. 2b, c). The CD4^{+}CD8^{+} DP thymocytes and DN2 populations also decreased in number within *Cellophane* thymocytes (Fig. 2b, c). In the LN and spleen, the percentages of

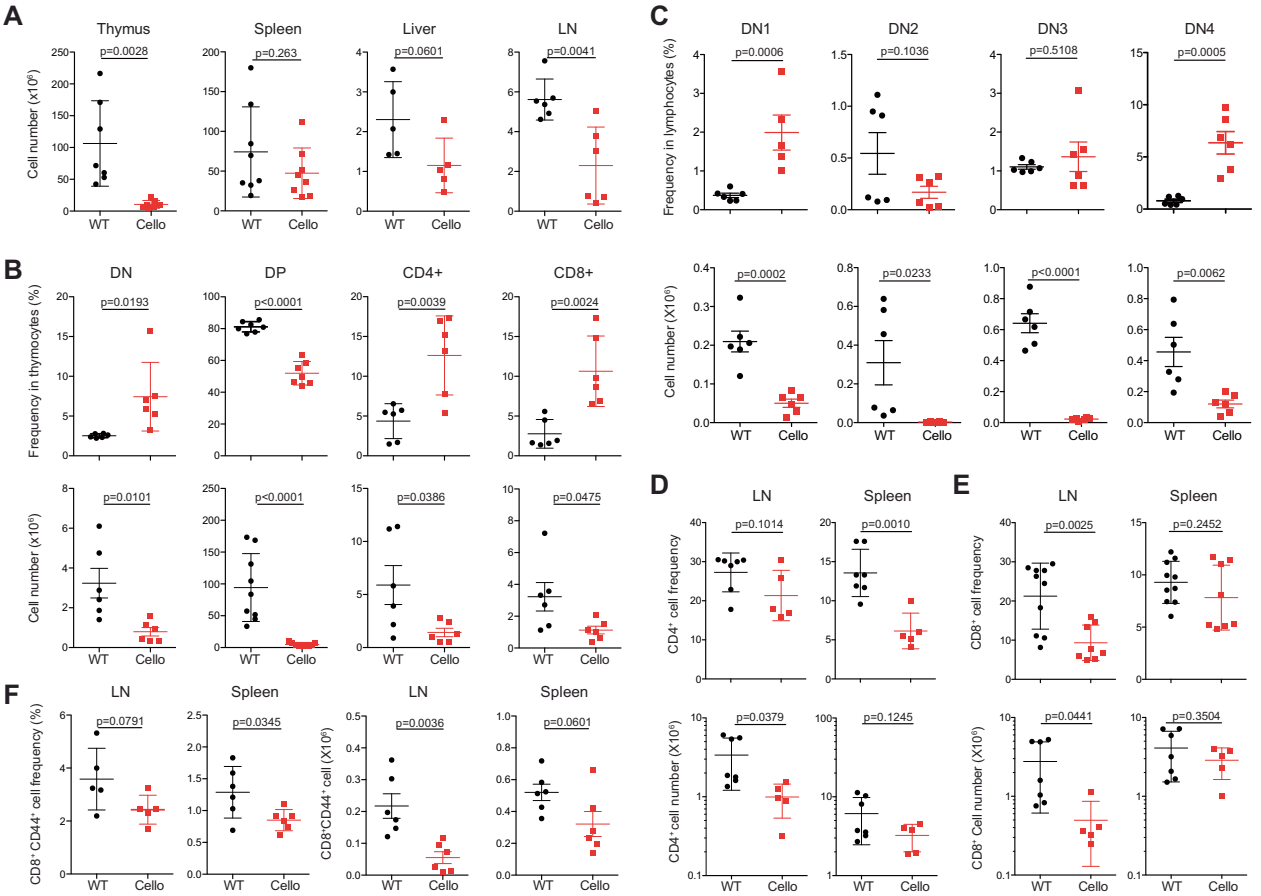

Fig. 2 Cellularity and proportions of T cell subsets in *Cellophane* mice. **a** Total number of cells from the thymus, spleen, liver, and LN. **b** Percentages and absolute numbers of the indicated T cell subsets (DN, DP, CD4 SP, and CD8 SP) in the thymus. **c** Percentages and absolute numbers of the indicated DN subsets defined by CD44 and CD25 expression in the thymus. Percentages and absolute numbers of (**d**) CD4 T cells and (**e**) CD8 T cells. (**f**) Percentages and absolute numbers of $CD8^+$ $CD44^+$ memory T cells in LN and spleen. Each dot represents an individual mouse. Data were pooled from 7 to 8 mice in four experiments (**a**–**e**) or three to six mice in two experiments (**f**). The statistical analysis was performed using an unpaired Student's *t* test

CD4 T cells and CD8 T cells were reduced (Fig. 2d, e), and the proportion of memory-phenotype $CD44^+$ T cells among total CD8 T cells was decreased by nearly 30% (Fig. 2f).

We then investigated the development of unconventional T cell subsets. We observed a drastic decrease in the proportion and in the number of iNKT cells as well as $NK1.1^+$ γδ T cells in *Cellophane* mice compared with those in littermate controls (Fig. 3a–d). This decrease affected all organs in *Cellophane* mice (Fig. 3a–d). iNKT cells were mainly affected at stage 3 (Fig. 3e). To complete our analysis, we also studied memory-phenotype $Ly49^+$ CD8 T cells, which are thought to arise "naturally" in the thymus without antigenic exposure.[33] All $Ly49^+$ CD8 T cell populations were dramatically reduced in LN and spleen from *Cellophane* mice in terms of both proportions and numbers, irrespective of the inhibitory Ly49 receptor type that was analyzed (Ly49A, Ly49F, or Ly49G2) (Fig. 3f, g).

Altogether, these data confirm the important role of Zeb1 in early T cell development. We also demonstrated the essential and specific role of Zeb1 in the development of peripheral T cell subsets expressing NK cell markers, such as iNKT cells, $NK1.1^+$ γδ T cells and $Ly49^+$ CD8 T cells.

Intrinsic role of *Zeb1* in thymic progenitors and T cell development

Zeb1 is also required for the development and expression of nonhematopoietic tissues and cell types.[20] To test whether Zeb1 played an intrinsic role in T cell development, we generated chimeric mice by transplanting sublethally irradiated Ly5a (CD45.1) mice with BM from *Cellophane* (CD45.2) or "WT" Ly5a x C57BL/6 (CD45.1/2) mice. In the thymus of chimeric mice, the proportions of DN2 and DP cells were dramatically decreased in *Cellophane* BM-transplanted mice compared with those in WT BM-transplanted mice, while the proportions of other cell populations defined by CD4 and CD8 were increased (Fig. 4a). The iNKT and $Ly49^+$ T cell subsets were also dramatically decreased in the peripheral organs of *Cellophane* → Ly5a BM chimeric mice compared with those of WT → Ly5a chimeric mice, indicating that *Zeb1* intrinsically regulated T cell development (Fig. 4b, c). The number of cells in all thymic T cell subsets and the numbers of peripheral iNKT cells and Ly49+ T cells were decreased in *Cellophane* → Ly5a BM chimeric mice compared with those in WT → Ly5a chimera mice (Fig. S2). $NK1.1^+$ γδ T cells were not analyzed because many of them are derived from fetal precursors[34] and were not reconstituted in BM chimera mice. To further test the role of Zeb1 in the environment of developing T cells, we also generated different BM chimeric mice using WT and *Cellophane* mice as both BM recipients and donors (WT → WT, WT → *Cellophane*, *Cellophane* → WT, and *Cellophane* → *Cellophane*). As shown in Fig. S3A, B, the proportions and numbers of the DN and DP cells subsets were determined by the genotype of the BM donor rather than that of the recipient. Similar conclusions could be reached upon examination of the proportion and number of iNKT cells in the thymus and the liver (Fig. S3C).

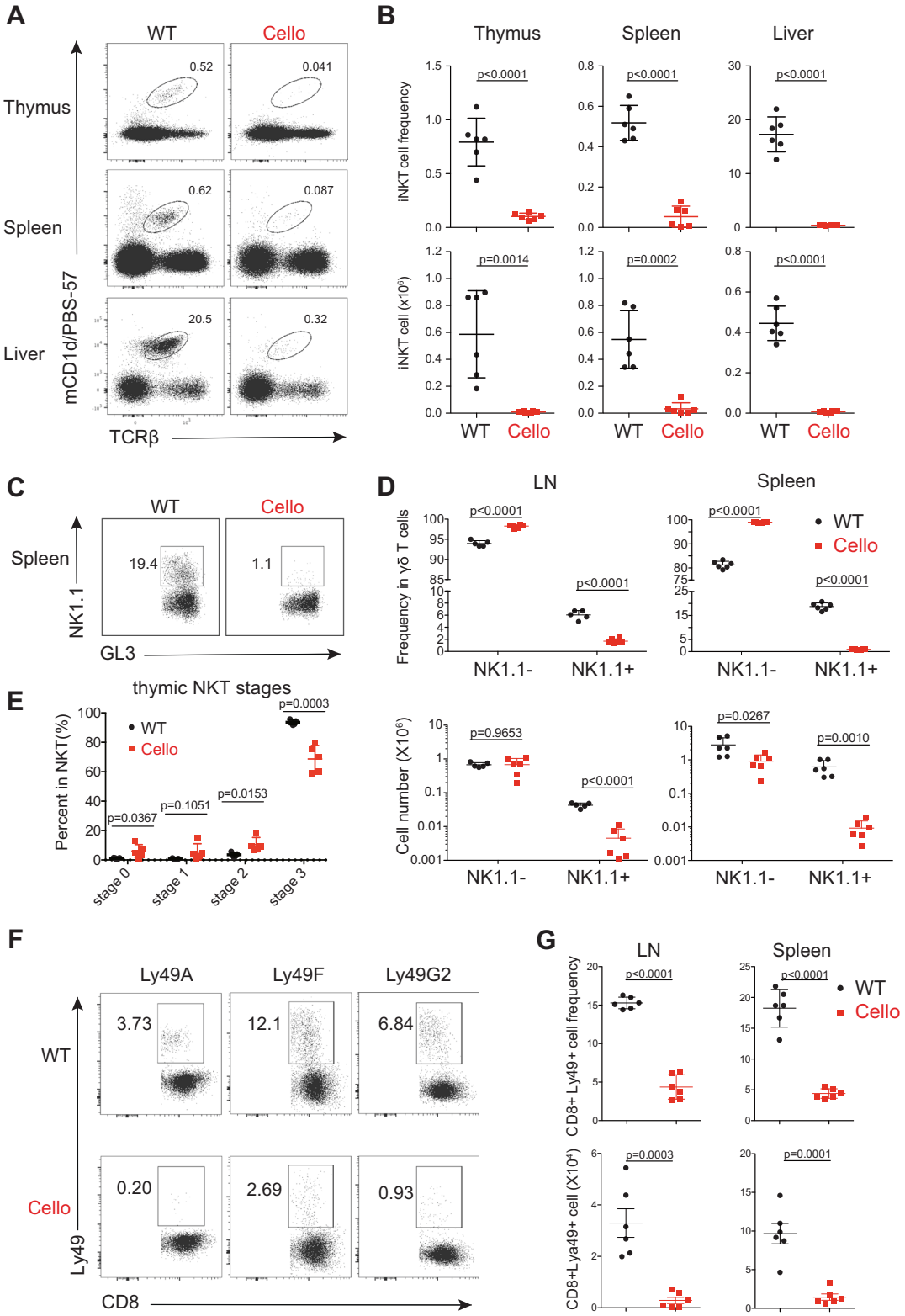

Fig. 3 *Cellophane* mice have decreased numbers of thymic DP cells and lack iNKT cells, NK1.1$^+$ γδ T cells and Ly49$^+$ CD8 cells. **a** Flow cytometry analysis of CD1d-tet$^+$ iNKT cells (black gate) from thymus, spleen, and liver in wild-type (WT) and *Cellophane* (Cello) homozygous mice as indicated. **b** Percentages and absolute numbers of iNKT cells (mCD1d/PBS-57$^+$ TCRβ$^+$) in the thymus, spleen, and liver. **c** Flow cytometry analysis of NK1.1$^-$ and NK1.1$^+$ γδ T cells (black square gates) from the spleen of WT and *Cellophane* mice. **d** Percentages within total γδ T cells and absolute numbers of NK1.1$^-$ and NK1.1$^+$ γδ T cells in spleen and LN. **e** Percentage within total thymic iNKT cells of cells from stages 0–3, as defined by CD24, CD44, and NK1.1 expression. **f** Flow cytometry analysis of CD8$^+$ CD44$^+$ Ly49A$^+$/Ly49F$^+$/Ly49G2$^+$ T cells (black square gates) from LN and spleen from WT and *Cellophane* mice. **g** Percentage within CD8$^+$CD44$^+$ T cells and absolute number of CD8$^+$ CD44$^+$ Ly49$^+$ T cells in spleen and LN. Each dot represents an individual mouse. Data are representative of two to four independent experiments with six mice in total in each panel. The statistical analysis was performed using an unpaired Student's *t* test

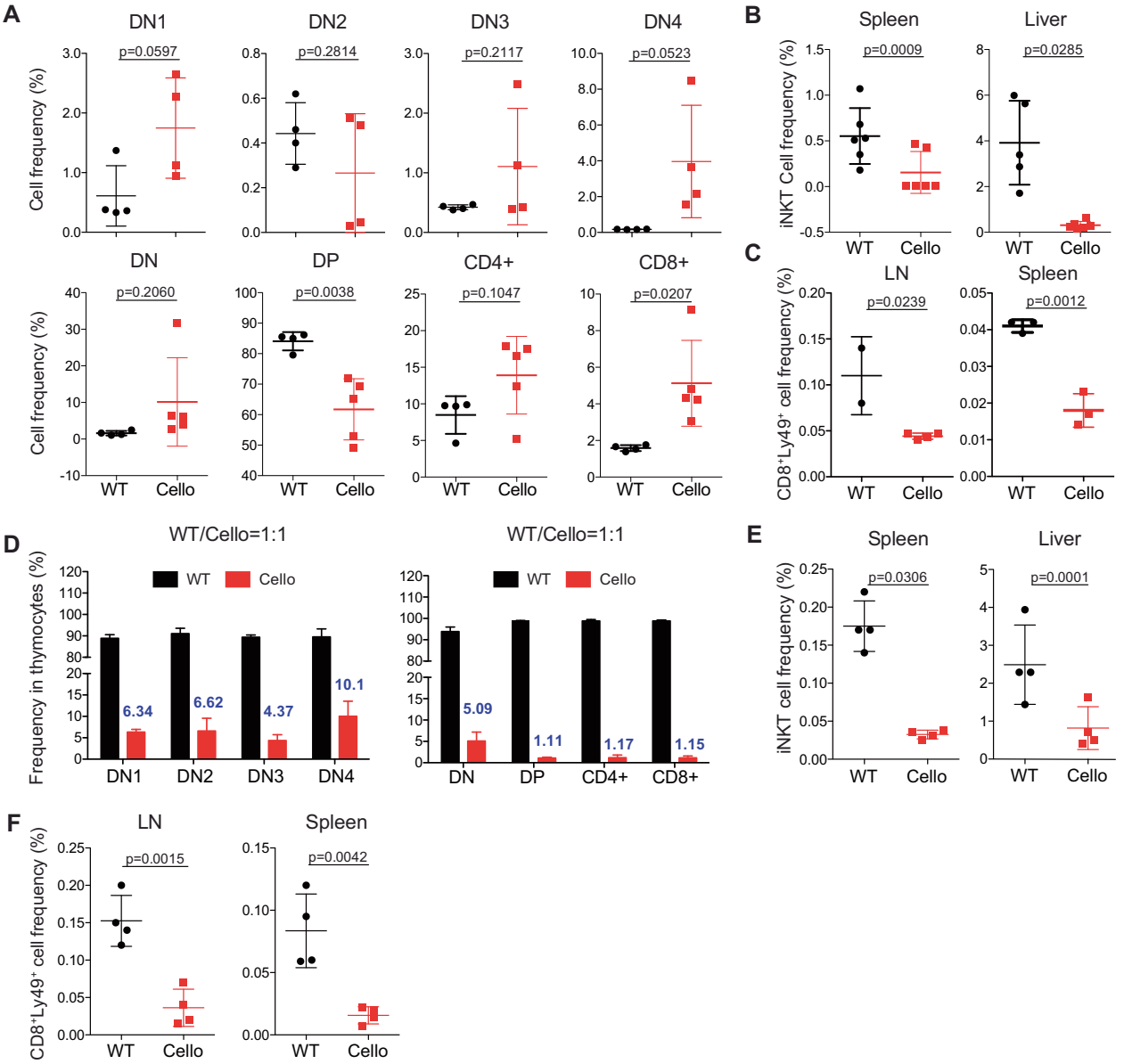

Fig. 4 The role of Zeb1 in T cell development is cell-intrinsic. **a** Flow cytometry analysis of the indicated thymocyte subsets from BM chimeras. Frequencies are shown for each subset. Recipients were Ly5a mice (CD45.1), and the donor BM was obtained from either Ly5a x C57BL/6 (CD45.1/2) or *Cellophane* (CD45.2) mice. **b** iNKT cell and **c** $CD8^+$ $Ly49^+$ T cell frequencies in the spleen, liver, or LN from the same BM chimera described in **a**. (**d**) DN1-4, DP, $CD4^+$, and $CD8^+$ cell reconstitution in the thymus of competitive BM chimeras. Recipients were Ly5a mice (CD45.1), and the donor BM was a 1:1 mix of cells from Ly5a x C57BL/6 (CD45.1/2) and *Cellophane* (CD45.2) mice. Eight weeks after BM transplantation, the cells were analyzed by flow cytometry. The number above the red bar shows the percentage of the indicated cells originating from *Cellophane* BM. **e**, **f** Frequencies of iNKT cells (**e**) and $Ly49^+$ cells within $CD8^+$ $CD44^+$ T cells in spleen, liver or LN from chimera BM described in **d**. Each dot represents an individual mouse. The results show the pooled data from two to three independent experiments for a total of two to six mice per group in each panel. Statistical analyses were performed using an unpaired Student's *t* test

We then generated mixed BM chimeras by transplanting lethally irradiated Ly5a mice with a 1:1 mixture of BM from *Cellophane* and Ly5a x C57BL/6 (WT) mice.

Cellophane T cell progenitors showed poor competitive fitness in BM chimeric mice (Fig. 4d). Indeed, the percentage of cells originating from the *Cellophane* BM progenitors was already low in the DN stage and further decreased during the transition between the DN and DP stages (Fig. 4d). In the periphery of mixed BM chimeric mice, we found that the proportions of iNKT and $Ly49^+$ CD8 T cells were greatly reduced among *Cellophane* T cells compared with those among WT lymphocytes (Fig. 4e, f), thus revealing that the role of Zeb1 in T cell development is cell-intrinsic and is not due to a defective stromal environment. Of note, we also analyzed the reconstitution of myeloid cells as a control. In the spleen, on average, 20% of macrophages, 25% of dendritic cells, and 28% of neutrophils originated from *Cellophane* mice (Fig. S3D), suggesting that Zeb1 regulated the development of all hematopoietic subsets, perhaps by regulating multipotent progenitors. However, the most important effects were observed for thymocytes and peripheral T cell subsets expressing NK cell markers.

Reduced survival and proliferation of *Cellophane* DN2 and DP cells
The decreased cellularity of the *Cellophane* thymi could be due to the reduced proliferation or increased apoptosis of thymocytes. To address this point, we first compared the survival of WT and

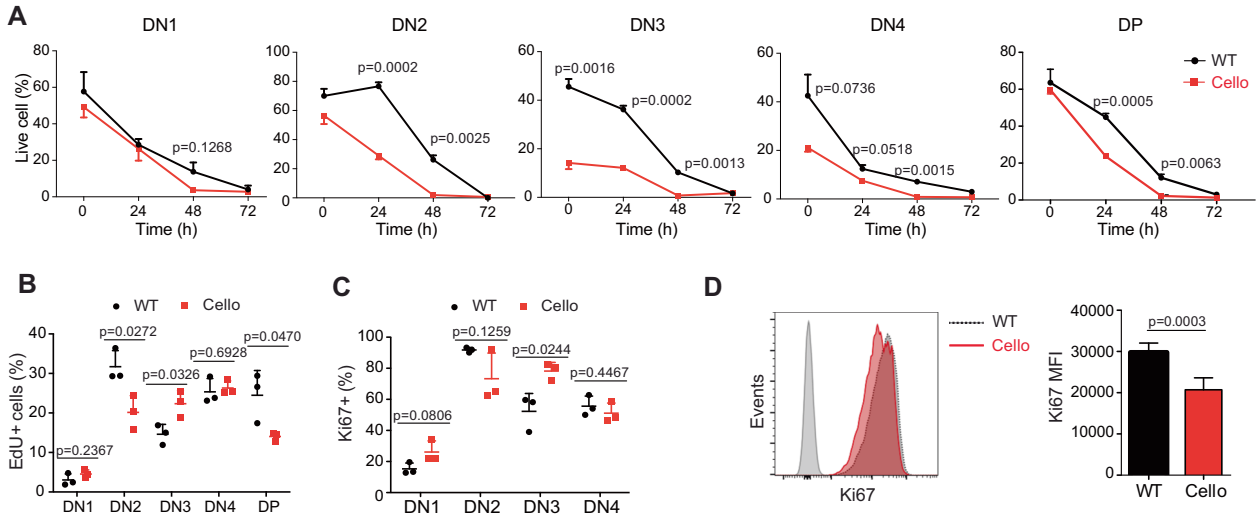

Fig. 5 *Cellophane* DP cells show reduced survival and proliferation. **a** Percentages of annexin-V-negative cells (live cells) among wild-type and *Cellophane* thymocytes cultured for 0–72 h. Each graph shows a different subset, as indicated. **b** EdU incorporation in wild-type and *Cellophane* thymocytes after a 12-h in vivo pulse of 0.2 mg EdU. **c** Frequencies of $Ki67^{+}$ cells in DN1-4 cell subsets from WT and *Cellophane* mice. **d** Ki67 nuclear staining in DP thymocytes from WT and *Cellophane* mice. Bar graphs (right panel) show the mean ± SD fluorescence intensity (MFI). Each dot represents an individual mouse. Data are pooled from three independent experiments with three mice in each group (**a**–**d**). Statistical analysis was performed using an unpaired Student's *t* test

Cellophane thymocytes during ex vivo culture. We found that *Cellophane* thymocytes in DN2, DN3, and DN4 showed reduced ex vivo viability compared with their WT counterparts (Fig. 5a). Moreover, after 24 or 48 h in culture, *Cellophane* DN2, DN3, DN4, and DP cells also showed reduced viability compared with control cells (Fig. 5a).

Next, we compared the in vivo proliferation of WT and *Cellophane* thymocytes, as measured by EdU incorporation. *Cellophane* DN2 and DP cells showed less proliferation than their WT counterparts, while *Cellophane* cells proliferated more than WT DN3 cells (Fig. 5b). Ki67 staining corroborated the data we obtained by using EdU incorporation (Fig. 5c, d). As all DP cells were Ki67 positive, we only reported the changes in the mean fluorescence intensity (MFI) (Fig. 5d).

Thus, the *Cellophane* mutation affects both the survival and proliferation of developing DN2 and DP thymocytes, which could account for the decreased number of such cells in the *Cellophane* thymi.

Zeb1 modulates TCR signaling strength

To gain insight into the mechanism of Zeb1 function, we focused on DP cells, as they expressed the highest level of Zeb1 among thymocytes (Fig. 1a). We first compared the expression of membrane proteins involved in thymocyte selection in *Cellophane* versus WT DP cells by flow cytometry. *Cellophane* DP cells expressed higher levels of Cd69, Cd25, and Cd5 than WT thymocytes (Fig. 6a). Nur77 is an early response gene expressed in T cells within hours after TCR stimulation. We observed an increase in the intracellular expression of Nur77, which was more highly correlated with Tcrβ levels in *Cellophane* cells than in WT DP thymocytes (Fig. 6a). Notably, similar levels of Cd4 and Cd8 were detected (Fig. 6a).

Next, we focused our attention on thymic iNKT cell subsets. The mouse thymi is known to contain at least three iNKT subsets, iNKT1, iNKT2, and iNKT17, which are thought to play distinct roles in the immune response.[35] iNKT1 cells comprise mainly stage 3 iNKT cells. TCR signaling strength governs the development of iNKT cell subsets in the thymus, in which high signaling strength is necessary for iNKT2 and iNKT17 development.[9,10] We examined iNKT cell subsets by staining for Plzf and Rorγt[36] in *Cellophane* mice and WT mice. The results in Fig. 6b show a significant increase in the proportions of iNKT2 and iNKT17 cells and a decrease in the proportion of iNKT1 cells in *Cellophane* mice compared with those in control mice. These data indicated an increase in the TCR signaling from DP progenitors of iNKT cells in *Cellophane* mice. The change in iNKT subsets was associated with subtle changes in the TCR repertoire, as assessed by measuring the frequencies of Vβ8-, Vβ7-, and Vβ2-positive cells among iNKT cells of each genotype. We observed a twofold increase in Vβ7 in *Cellophane* mice (Fig. 6c). This could reflect the increase in iNKT2 cells, as a previous study showed that Vβ7 was more often associated with iNKT2 cells.[9] Thymic *Cellophane* iNKT cells expressed normal levels of the TFs T-bet and Egr2 but strongly reduced levels of Cd4 (Fig. 6d). Since CD4 is known to sustain TCR signaling strength,[5] the selection of $CD4^{low}$ iNKT cells in *Cellophane* mice could reflect the adaptation to overt TCR signaling in *Cellophane* DP cells.

We then specifically analyzed TCR signaling in developing thymocytes. We started by measuring the phosphorylation (p) levels of a series of signaling proteins involved in TCR-mediated activation, either at the steady-state in freshly isolated thymocytes or following TCR engagement by cross-linking with anti-CD3 antibodies. To minimize the experimental variation, we used a barcoding strategy that allowed stimulation and then staining of WT and *Cellophane* thymocytes simultaneously (see "Materials and methods"). The results in Fig. 6e, f show increases in pAkt (Ser473), ribosomal protein pS6, and, to a lesser extent, pErk either at the steady-state or following TCR engagement in *Cellophane* DP cells compared with WT DP cells. Thus, the MAPK and PI3K/Akt pathways are more active in thymocytes undergoing selection in *Cellophane* mice compared with those in control mice. To complement this analysis, we also assessed the calcium response of DP cells of both genotypes in response to TCR engagement. As shown in Fig. 6g, h, this response was stronger for *Cellophane* DP cells than control DP cells in terms of both intensity (peak) and duration (area under the curve, AUC). Thus, Zeb1 modulates the signaling strength downstream of the engaged TCR at the DP stage, and *Cellophane* DP cells show increased TCR signaling, which may increase negative selection and therefore account for defective T cell development in *Cellophane* mice. We also measured pre-TCR signaling in DN cells following stimulation with anti-CD3 antibodies. This analysis did not reveal any difference between WT and *Cellophane* DN cells (data not shown).

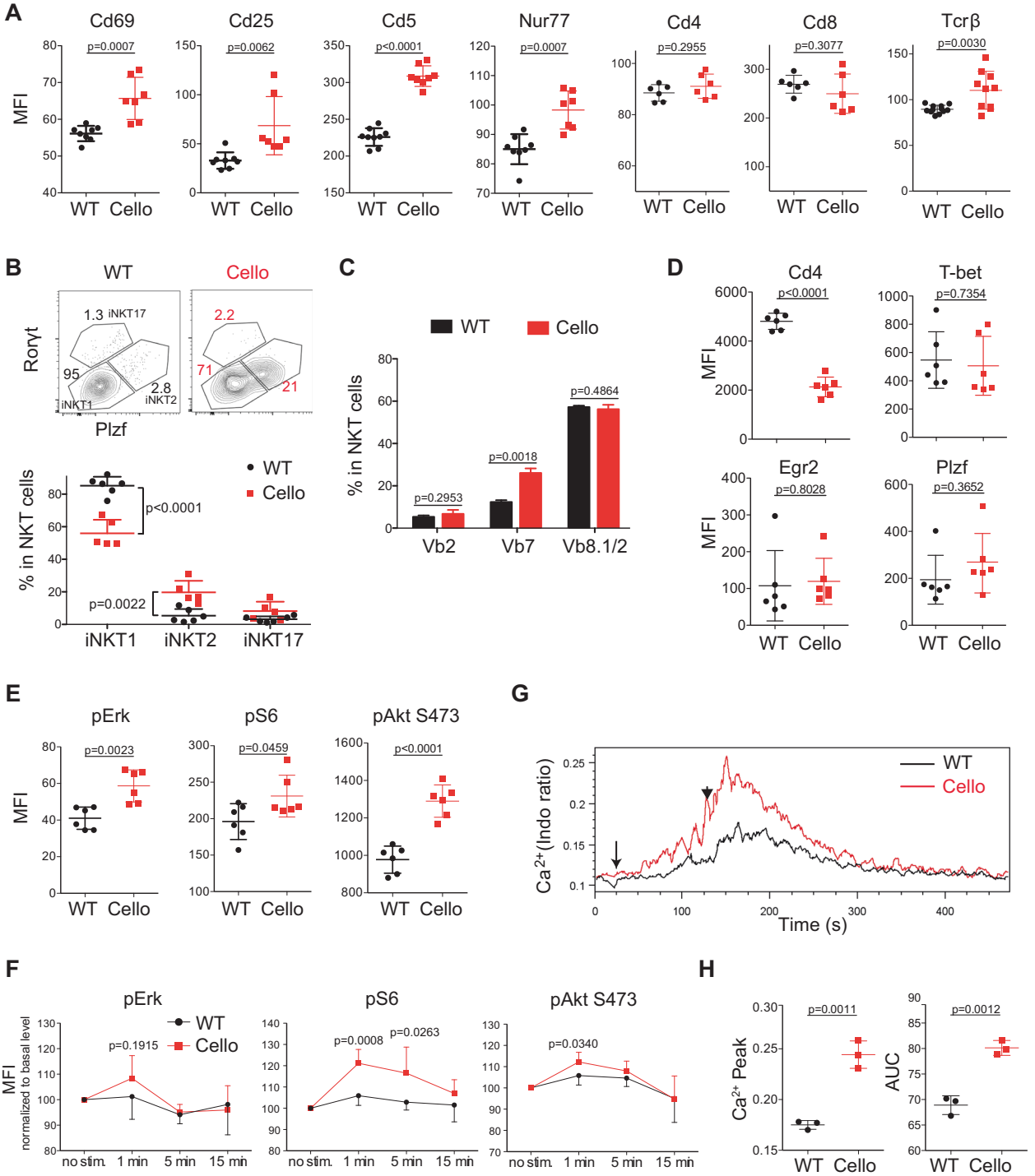

Fig. 6 *Cellophane* DP thymocytes display increased TCR signaling. **a** Flow cytometry analysis of Cd69, Cd25, Cd5, Nur77, Cd4, Cd8, and Tcrβ expression (mean fluorescence intensity) in DP thymocytes of wild-type and *Cellophane* mice. **b** Left panels: Representative flow cytometry analysis of iNKT1 (Plzf lo, Rorγt-, T-bet+), iNKT2 (Plzf hi, Rorγt-, T-bet-), and iNKT17 (Plzf int, Rorγt+, T-bet-) cell subsets in wild-type and *Cellophane* mice (as defined by the gating strategy shown in the upper panel). Right panel: graphs of the percentages of iNKT cell subsets within total iNKT cells. **c** The TCRVβ repertoire of thymic iNKT cells was analyzed by flow cytometry. Bar graphs show the mean ± SD frequencies of individual Vβ chains within iNKT cells. **d** Expression of Cd4, T-bet, Egr2, and Plzf in iNKT cells as measured by flow cytometry (mean fluorescence intensity). **e** Phosphorylation levels of Erk, S6, and Akt (S473) in resting DP thymocytes from WT and *Cellophane* mice. **f** Phosphorylation levels of Erk, S6, and Akt (Ser473) in DP cells stimulated with anti-CD3 antibody for the indicated times. The results are normalized to the nonstimulated condition (i.e., basal level is 100%) for each group. **g** Representative histogram overlay showing the Ca^{2+} flux in thymic DP cells from wild-type or *Cellophane* mice stimulated with anti-CD3 antibodies, as measured by flow cytometry. Thymocytes were activated following incubation with biotinylated anti-CD3 (arrow) followed by cross-linking with streptavidin (arrowhead). **h** Dot plots showing the AUC (area under the curve) and Ca^{2+} peak. Statistical analysis was performed using an unpaired Student's *t* test. Each dot represents an individual mouse. Data are pooled from three experiments with a total of eight mice in each group (**a**), three experiments with six mice (**b**), three mice (**c**), two experiments with six mice (**d**–**f**) or three experiments with three mice (**g**, **h**)

Zeb1 broadly shapes transcription during the DP → SP transition to promote proliferation and repress TCR signaling

To further uncover the mechanisms of Zeb1 function during T cell development, we performed RNA-seq to compare the WT and *Cellophane* DP transcriptomes. We found 538 differentially expressed genes (DEGs, p value < 0.05, log2-fold change > 1). A total of 204 genes were increased, and 334 were downregulated in *Cellophane* DP cells compared with WT DP cells. These data reveal that Zeb1 broadly shapes the genetic program of developing thymocytes (Fig. 7a and Table S1). For some of the DEGs identified, antibodies were available, and we were thus able to confirm the higher expression of Foxo1, Ms4a4b, Itgb7, Ccr7, and Ccr4 in *Cellophane* cells compared with that in control DP cells; in contrast, we observed lower Cd81 expression in *Cellophane* DP cells than in WT cells (Fig. 7b).

Next, we queried the ImmGen database to retrieve the expression profile of the Zeb1-regulated gene set (induced or repressed) across all thymocyte subsets. Interestingly, genes downregulated in *Cellophane* DP cells (i.e., normally induced by Zeb1) correspond to genes that are normally expressed at high levels in early T cell progenitors and at low levels in mature T cells (Fig. 7c). Their expression level normally drops during the DP to SP transition, which is when Zeb1 is highly expressed. Genes upregulated in *Cellophane* DP cells correspond to genes that show a reciprocal pattern of expression (Fig. 7c). This pattern of expression also correlates with cell proliferation and TCR responsiveness in thymocytes. Indeed, irrespective of the mouse genotype, SP T cells are much more responsive to TCR signaling-mediated calcium responses than DP cells but also do not cycle as much as DP cells (data not shown). This suggests that Zeb1 promotes cell proliferation and represses TCR signaling specifically at the DP stage, presumably to ensure proper selection.

A functional annotation analysis of DEGs identified by our RNA-seq analysis using "Metascape"[37] highlighted the cell cycle as the most downregulated biological process in *Cellophane* DP cells compared with control DP cells (Fig. 7d and Table S2), confirming the findings in Fig. 3. Pathways linked to Ifnγ (and also type I-Ifn; Table S2), antigen presentation, leukocyte differentiation, and apoptosis were significantly associated with genes upregulated in *Cellophane* DP cells compared with those in WT cells (Fig. 7d). Of note, a modest but significant enrichment of genes involved in the calcium response was also associated with these upregulated genes, corroborating the data shown in Fig. 6. To further annotate this dataset, we performed individual PubMed searches to look for connections between genes upregulated in *Cellophane* DP cells compared with control DP cells and "T cell activation", "TCR signaling", or "T cell development". Interestingly, this analysis showed that more than 25% of the genes in the list played a known role in T cell activation or TCR signaling, and 10% played a role in T cell development, as defined using loss-of-function mouse strains (Table S3). Moreover, we used the STRING database of physical and functional protein interactions[38] to further annotate genes that were up- or downregulated in *Cellophane* DP cells compared with control DP cells. In particular, we used the PubMed module that searches for the enrichment of gene lists in articles in PubMed. This unbiased analysis showed that genes upregulated in *Cellophane* DP cells were significantly enriched for genes involved in negative selection[39] or T cell maturation regulated by Bcl11b[40] (Table S4), which corroborated our manual PubMed searches.

Chromatin regions remodeled at the DP stage contain Zeb1 binding motifs

Next, we wanted to determine whether Zeb1 could regulate chromatin remodeling at the DP stage of T cell development. For this, we took advantage of a recently published large-scale analysis of chromatin accessibility and gene expression across 86 immune cell subsets, including subsets representing T cell developmental stages in the thymus.[41] In this study, in silico predictions identified Zeb1 as one of the few TFs whose expression was correlated with modifications of chromatin accessibility during thymic T cell development and for which the corresponding chromatin regions contained sites predicted to be bound by Zeb1. Other TFs in this category included Gata3, Tcf7, Lef1, Tcf12, and Zfp740 (Fig. S4A), especially Tcf7 and Tcf12, whose roles in T cell development have been well established.[32] We retrieved the open chromatin regions (OCRs) for which Zeb1 motifs were discovered in this study and whose accessibility changed during T cell development (see the corresponding clusters in Fig. S4B) and compared the list of corresponding genes with the DEGs between *Cellophane* and WT DP cells identified in our own study. We found an important overlap between both lists that included many of the genes previously highlighted in our analysis (Fig. 7e, p value = 1.839413e−46). Altogether, these data suggest that Zeb1 is a direct transcriptional regulator of T cell development that is especially involved in the DP to SP transition that promotes cell proliferation and ensures proper selection.

DISCUSSION

Here, we demonstrated that Zeb1 is essential for the transition through the DN2 and DP stages of T cell development as well as for the differentiation of iNKT cells, NK1.1$^+$ γδ T cells and Ly49$^+$ CD8 T cells. Mechanistically, Zeb1 regulates the expression of a number of genes that are notably involved in cell proliferation or in TCR signaling at the DP stage. In *Cellophane* mice, these events may perturb thymic development and selection in a way that does not allow the production of the NK1.1$^+$ and Ly49$^+$ T cell subsets.

Zeb1 expression was found to increase at the DN2 stage and to be maximal at the DP stage of T cell development. Accordingly, we found decreases in the frequencies of DN2 and DP thymocytes in *Cellophane* mice. This could be due to the cell-intrinsic role of Zeb1 in DN2 and DP proliferation. A number of genes involved in the cell cycle were differentially expressed between WT and *Cellophane* DP cells, as revealed by our RNA-seq analysis. There is also a strong link in the literature between Zeb1 and cell proliferation in cancer. In particular, Zeb1 interacts with many TFs involved in the regulation of cell growth, such as Smad TFs, which are downstream of several growth factor pathways.[22] Moreover, Zeb1 is known to repress cyclin-dependent kinases during EMT.[21] However, the levels of CDkn2c and CDkn3 were decreased by Zeb1 in DP thymocytes, suggesting the different roles of Zeb1 in epithelial versus lymphoid cells. The decreased proliferation of DN2 and DP cells is expected to have important consequences for overall thymic output. Indeed, we found decreased numbers of peripheral T cells in *Cellophane* mice. However, this defect was much more pronounced for iNKT cells, NK1.1$^+$ γδ T cells, and Ly49$^+$ CD8 T cells. In particular, iNKT cells were virtually absent from the periphery. The altered development of T cells was associated with increased TCR signaling at the DP stage, which was verified by increased basal levels of Cd5 and Nur77 and increased mTOR activity and calcium flux upon CD3 engagement. iNKT cells are known to receive stronger TCR signals than conventional T cells during their development.[6] Thus, increased TCR signaling in *Cellophane* DP cells could trigger cell death via negative selection of iNKT precursors. The increased negative selection of iNKT cells has already been shown to occur in mice in which transgenic TCR-β chains confer high affinity for self-lipid/CD1d complexes when they are randomly paired with Vα14-Jα18 rearrangements.[42] Thus, increased negative selection could impair the development of iNKT cells in *Cellophane* mice and perhaps that of other T cell subsets expressing NK cell markers. Indeed, strong TCR-mediated signals are also important for γδ T cell development.[43,44] In particular, NK1.1$^+$ γδ T cells have an oligoclonal TCR repertoire and accumulate in mouse models of decreased TCR signaling,[45] suggesting that this subset of γδ cells

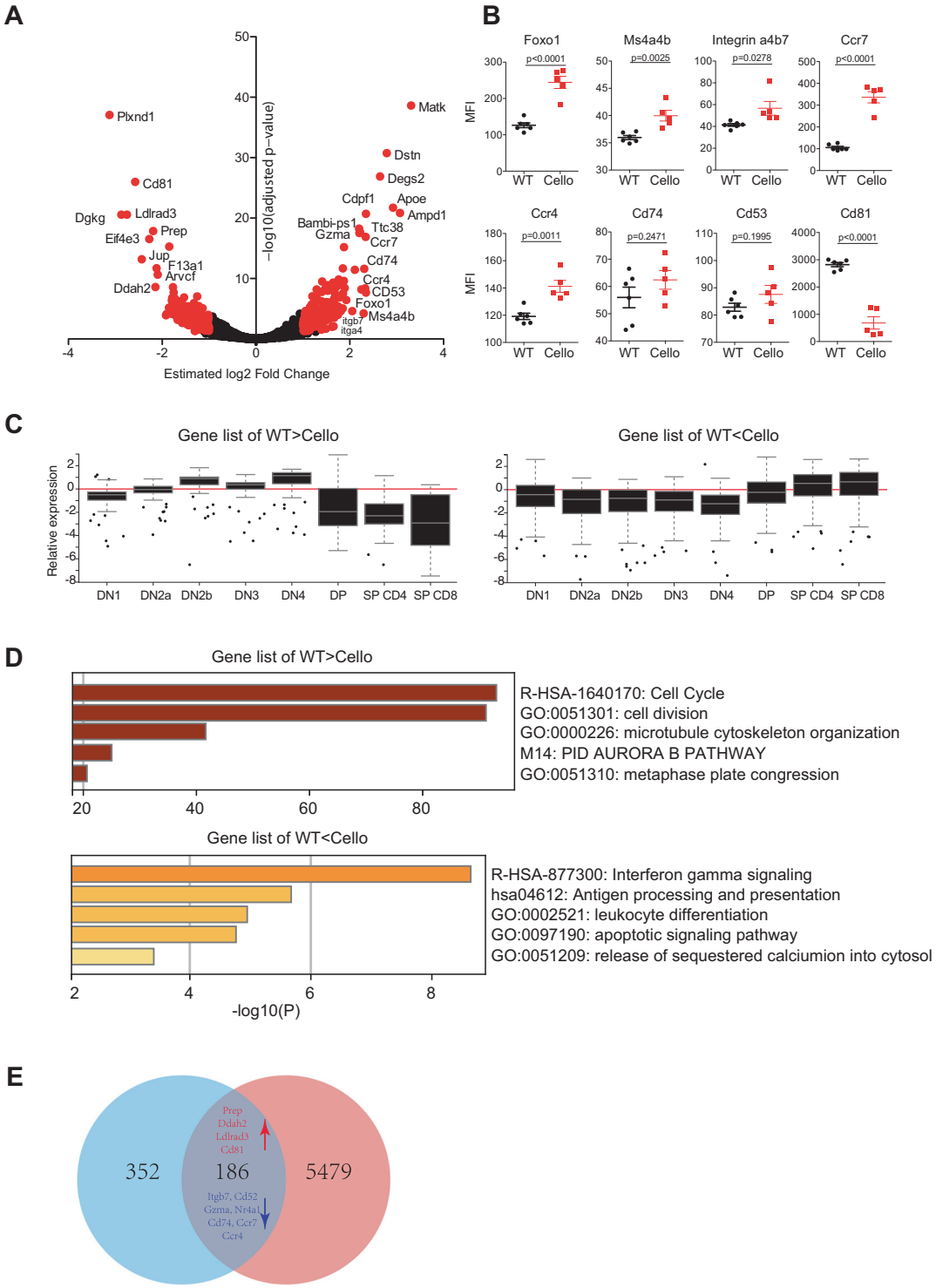

Fig. 7 RNA-seq analysis of *Zeb1*-regulated genes. **a** Volcano plot representing the −log10 adjusted *p* value as a function of the estimated log2-fold-change. Significant genes were selected using the following thresholds: an adjusted *p* value lower than 0.05 and an absolute value of the log2-fold-change greater than 1. For significant genes (plotted in red), a selection of the gene names is displayed. The results are representative of the biological replicates in each group. **b** Flow cytometry analysis of several genes identified by RNA-seq as either upregulated (Foxo1, Ms4a4b, integrin α4:β7, Ccr7, Ccr4, Cd74, and Cd53) or downregulated (Cd81) in *Cellophane* mice. Data are pooled from two independent experiments with a total of six mice. **c** Expression level of genes in two selected lists (200 genes in each list) that were either upregulated (WT < Cello) or downregulated (WT > Cello) in different αβ T cell subsets in *Cellophane* mice with a fold change > 2 and a *p* value < 0.05, as indicated. Graphs are adapted from the ImmGen website. **d** Pathway analysis of DEGs in **a** using Metascape. The selected terms are shown among the most significant terms. **e** Venn diagram showing the overlap between DEGs in **a** and genes located within 100 kb of OCRs containing Zeb1 motifs for which chromatin accessibility changed during T cell development (the corresponding clusters are visualized in Fig. S4B). The genes upregulated in WT mice are shown in red, while the genes that were downregulated are shown in blue

can also be negatively selected. The ontogeny of Ly49$^+$ CD8 T cells is not very well known, but our data suggest that their development and selection could share common mechanisms with those of NK1.1$^+$ T cells. How does Zeb1 regulate TCR signaling strength? *Cellophane* DP thymocytes expressed higher levels of Tcrβ than control DP thymocytes, and this could certainly lead to increased TCR signaling. Moreover, the RNA-seq analysis we performed suggested that there were multiple connections between Zeb1 and signaling transduction through the TCR. For example, multiple members of the GTPases of the IMmunity-Associated Proteins (GIMAP) family (GIMAP5 and GIMAP8) were upregulated in *Cellophane* DP cells. Interestingly, Gimap5 enhances calcium influx following TCR stimulation.[46] Several members of the Ms4a family of receptors, which have four transmembrane domains, are also upregulated in *Cellophane* DP cells and could reinforce TCR signaling. Indeed, the transduction of signaling by Ms4a4b in naive T cells can heighten their sensitivity to antigens through a process that could involve association with costimulatory molecules.[47] Several phosphatases and kinases are also deregulated in *Cellophane* DP cells and could perhaps alter TCR signaling. In particular, the expression of Pyk2 (encoded by *Ptk2b*), Rasgrp4, Rasl1, or Rasa3 could all contribute to increased TCR signaling via calcium flux or the MAPK pathway.

A series of TFs were also deregulated in *Cellophane* DP cells, which showed notable upregulation of JunB, Jun, Atf6, Foxo1, Stat4, or Irf7/9. JunB and Jun are essential components of AP-1 TFs and are typically activated downstream of TCR stimulation. Similar to Nur77, they could represent surrogate markers of increased TCR signaling in *Cellophane* DP. The derepression of Foxo1 could in part account for altered T cell development, as it regulates Ccr7, CD62L, and S1pr1 via Klf2.[48] The lack of control by Klf2 could perturb and perhaps even accelerate the normal migration of developing thymocytes in the medullary region where negative selection occurs. Foxo1 deletion in thymocytes was reported to decrease the number of DP thymocytes, and Foxo1-deficient peripheral T cells seem to be refractory to TCR stimulation through unknown mechanisms.[49] Moreover, upregulation of Foxo1 in *Cellophane* DP cells could in part explain the inverse changes in cell proliferation observed in these cells compared with those in control DP cells, since Foxo TFs are known to promote stem cell quiescence[50] and clearly contribute to the regulation of cell division, survival, and metabolism in T cells.[51] A recent study showed that the transcriptional repressor Gfi1 is important in maintaining Foxo1 expression at low levels in DP thymocytes.[52] In the absence of Gfi1, premature expression of genes normally expressed in mature T cells and accelerated maturation of DP cells into SP thymocytes occurred, which was largely attributable to Foxo1 derepression. Zeb1 and Gfi1 could therefore cooperate to repress Foxo1.

There are many similarities in the phenotypes of *Tcf12*-deficient[53] and *Cellophane* mutant mice, particularly in terms of the susceptibility of DP cells to cell death and the impaired development of iNKT cells. Moreover, microarray data from the ImmGen consortium suggest that Tcf12 and Zeb1 are strongly coregulated, and ATAC-seq data predict that they control chromatin accessibility during thymic T cell development together with Gata3, Tcf1, Lef1, and Zfp740 (Fig. S4 and ref. [41]). Altogether, these data suggest a strong functional link between Zeb1, Heb (encoded by *Tcf12*), and perhaps Tcf1, which acts in coordination with Heb.[32] The fact that Zeb1 is known to bind tandem E-box motifs suggests that there is possibly competition between Zeb members and E proteins for binding of those genes regulated by tandem E-boxes. Such competition has been previously established in the context of the CD4 enhancer, which is repressed by Zeb1, through competition with Heb for E-box binding.[54] Moreover, Zfh-1 and Daughterless, the *Drosophila* homologs of *Zeb1* and *Tcf12*, are also known to compete for the same genomic sites.[55] The deletion of *Tcf12* and *Tcf1* in thymocytes results in the opposite phenotype as the *Cellophane Zeb1* mutation in terms of DP proliferation.[32] This suggests that Heb and Zeb1 could have partially antagonistic activities in the regulation of genes bearing tandem E-box elements. Competition between Zeb1 and E proteins has already been suggested to play a role in the control of GATA3 expression in human CD4 T cells.[56] *Cellophane* mice express a truncated form of Zeb1 that is expressed at lower levels than WT Zeb1. As the phenotype of these mice is milder than that of *Zeb1*$^{-/-}$ mice, we assumed that the *Cellophane* mutation was hypomorphic. However, we cannot rule out that *Cellophane* Zeb1 may retain some DNA-binding capability and therefore act as a dominant negative molecule by preventing the binding of E-box proteins. Further work will be needed to precisely map the interactions between Zeb TFs and E proteins. The regulatory network may also include inhibitors of the differentiation genes Id2 and Id3, which are TFs that bind and inactivate E proteins, thereby regulating their function. Moreover, a deficiency in Id3 has the same impact on NK1.1$^+$ γδ T cells as a deficiency in TCR signaling,[45] which indicates a links between both factors.

The *Zeb1* genomic region is frequently deleted in cutaneous T cell lymphomas (CTCLs).[57] Such deletions are often associated with genetic mutations in components of the TCR signaling machinery (recurrent alterations in *Card11, Plcg1, Lat, Rac2, Prkcq, CD28,* and genes that encode calcium channel subunits). This observation, together with our own data showing the role of *Zeb1* in repressing TCR signaling, suggests that *Zeb1* deletion could promote lymphomagenesis by releasing the normal constraints on TCR signaling. Of note, a previous study proposed the essential role of IL-15 in CTCL development and showed that IL-15 expression was suppressed in patients with CTCL due to promoter hypermethylation and the failure of Zeb1 to gain access to and repress the IL-15 regulatory region.[58] However, IL-15 expression was not detected in developing thymocytes in our RNA-seq analysis, excluding the possibility that the IL-15 pathway could play a role in the mechanism of action of Zeb1 in T cell development. However, we found that the transcriptional responses to different cytokines, such as interferons or IL-6, were increased in *Cellophane* DP cells (Table S2). Zeb1 may therefore normally repress the responses to these cytokines, which presumably occurs to ensure proper selection. TGF-β is a known regulator of iNKT cell development[59] that promotes early differentiation and prevents the apoptosis of developing iNKT cells. A recent study showed that Zeb1 expression was induced by TGF-β in conventional CD8 T cells stimulated through the TCR and was essential for memory T cell survival and function.[30] Although we failed to detect any effect of recombinant TGF-β on *Zeb1* expression in thymocytes (data not shown), it would be interesting to address this question in vivo using appropriate genetic models.

In summary, Zeb1 is an essential member of the TF network that regulates T cell development and selection in the DN2 and DP stages. Furthermore, we have also shown that Zeb1 facilitates the development of iNKT cells and other T cell subsets expressing NK cell markers by regulating the cell cycle and TCR signaling in developing thymocytes.

MATERIALS AND METHODS

Mice

Mice that were 8–24 weeks old were used. Wild-type C57BL/6 mice were purchased from Charles River Laboratories (L'Arbresle). *Cellophane* mice were previously described,[28] and their littermates were used as controls. This study was carried out in accordance with the French recommendations in the Guide for the Ethical Evaluation of Experiments Using Laboratory Animals and the European guidelines 86/609/CEE. All experimental studies were approved by the local bioethics committee CECCAPP. Mice were bred at the Plateau de Biologie Expérimentale de la Souris (ENS, Lyon).

Bone marrow chimeric mice

8- to 10-week-old Ly5a mice or Ly5a x C57BL/6 mice were anesthetized with ketamine/xylazine before irradiation at a dose of 9 Gray with an X-ray irradiator XRAD-320. After irradiation, they were intravenously injected with $2–5 \times 10^6$ cells collected from either wild-type or mutant murine bone marrow or a mix of both (as indicated in the figures). Immune cell reconstitution was analyzed 8 weeks post BM injection.

Flow cytometry

Single-cell suspensions of thymus, spleen, and liver were used for flow cytometry. Cell viability was measured using annexin-V (BD Biosciences)/live-dead fixable (eBiosciences) stain. Intracellular staining for TFs was performed using a Foxp3 kit (eBioscience). Lyse/Fix and PermIII buffers (BD Biosciences) were used for intracellular staining of phosphorylated proteins. Flow cytometry was carried out on a FACS Canto, a FACS LSRII, or a FACS Fortessa (Becton-Dickinson). Data were analyzed using FlowJo (Treestar). Antibodies were purchased from eBioscience, BD Biosciences, R&D Systems, Beckman Coulter, Miltenyi, or Biolegend. We used the following antibodies: anti-mouse CD3 (clone 145-2C11), anti-mouse CD4 (clone GK1.5), anti-mouse CD8 (clone 53-6.7), anti-mouse TCRβ (clone H57-597), anti-mouse CD69 (clone H1.2F3), anti-mouse TCRγδ (clone GL3), anti-mouse NK1.1 (clone PK136), anti-mouse CD24 (clone M1/69), anti-mouse CD44 (clone IM7), anti-mouse CD27 (clone LG.7F9), anti-mouse TCRVβ2 (clone B20.6), anti-mouse TCRVβ7 (clone TR310), anti-mouse TCRVβ8.1/8.2 (clone KJ16-133), anti-mouse Ly49A (clone A1), anti-mouse Ly49E/F (clone REA218), anti-mouse Ly49G2 (clone 4D11), anti-mouse CD45.1 (clone A20), anti-mouse CD45.2 (clone 104), anti-mouse Nur77 (clone 12.14), anti-mouse Ccr7 (clone 4B12), anti-mouse CD5 (clone 53-7.3), anti-mouse CD81 (clone Eat-2), anti-mouse CD53 (clone OX79), anti-mouse Lpam-1 (clone DATK-32), anti-mouse Foxo1 (clone C29H4), anti-mouse Ms4a4b (clone 444008), anti-mouse CD74 (clone In1/CD74), anti-mouse T-bet (clone 4B10), anti-mouse Egr2 (clone erongr2), anti-mouse Plzf (clone Mags.21F7), anti-mouse Rorγt (clone AFKJS-9), anti-mouse pErk (clone 20A), anti-mouse pAkt (Ser473) (clone M89-61), and anti-mouse pS6 (clone D57.2.2E). For the staining of iNKT cells, phycoerythrin (PE)-conjugated PBS-57 loaded on mouse CD1d tetramers (mCD1d/PBS-57) was obtained from the Tetramer Core Facility of the National Institute of Health.

Measurement of in vivo cell proliferation and ex vivo survival

Mice were given one intraperitoneal injection of 0.2 mg EdU (BD Bioscience). Twelve hours after EdU injection, the mice were sacrificed, and the organs were harvested. Cells derived from the thymus were stained with the antibodies specific for the cell surface antigens described above. After fixation and permeabilization, cells were stained with FITC anti-EdU antibody and 7-AAD (BD Pharmingen) according to the manufacturer's instructions. EdU incorporation into different cell populations was measured by flow cytometry.

For the measurement of cell viability, we stained the thymocyte suspensions with 7-AAD and antibodies against annexin-V (BD Biosciences) and other surface markers, such as CD4, CD8, CD69, TCRβ, CD25, and CD44, either ex vivo or 24, 48, or 72 h after in vitro culture in complete medium.

Cell sorting and RNA preparation

Lymphocytes were obtained from the thymus. Immune cell populations, including DN1-4, DP, SP $CD4^+$ and $CD8^+$, and iNKT cells, were stained in combination with antibodies against the cell-specific markers CD4, CD8, CD69, TCRβ, CD25, CD44, and mCD1d/PBS-57 and were subsequently sorted into different subsets using a FACSAria Cell Sorter (Becton-Dickinson, San Jose, USA). The purity of the sorted cell populations was over 98%, as validated by flow cytometry. The sorted cells were lysed using TRIzol reagent (Invitrogen) or RLT buffer from the RNeasy Micro kit (Qiagen), and RNA was extracted according to the manufacturer's instructions.

Quantitative RT-PCR

We used a high capacity RNA-to-cDNA kit (Applied Biosystems, Carlsbad, USA) or iScript cDNA synthesis kit (Bio-Rad) to generate cDNA for RT-PCR. PCR was carried out with a SYBR Green-based kit (FastStart Universal SYBR Green Master, Roche, Basel, Switzerland) or SensiFast SYBR No-ROX kit (Bioline) on a StepOne plus instrument (Applied Biosystems, Carlsbad, USA) or a LightCycler 480 system (Roche). Primers were designed using software from Roche. We used the following primers for mouse QPCR: Zeb1 forward primer, 5′-GCCAGCAGTCATGATGAAAA-3′; Zeb1 reverse primer, 5′-TATCACAATACGGGCAGGTG-3′; Zeb2 forward primer, 5′-CCAGAGGAAACAAGGATTTCAG-3′; Zeb2 reverse primer, 5′-AGG CCTGACATG

TAGTCTTGTG-3′; Gapdh forward primer, 5′-GCATGGCCTTCCGTG TTC-3′; Gapdh reverse primer, 5′- TGTCATCATACTTGGCAGGTTTC T-3′. The relative expression of Zeb1 and Zeb2 were normalized to Gapdh expression.

Western blotting

Cells were lysed in NP40 lysis buffer (20 mM Tris, HCl pH 7.4; 150 mM NaCl; 2 mM EDTA; 1% NP40) containing protease inhibitors for 30 min on ice. The supernatant was collected following 10 min of centrifugation at 12,000 *g* at 4 °C, and the protein concentration was quantified by a μBCA quantification kit (Thermo Fisher Scientific). Fifty micrograms of total cellular protein from the thymus was incubated for 5 min at 95 °C. Protein samples were separated by electrophoresis using Novex 4–12% Tris-Glycine gels (Life Technologies) for 1 h at 120 V. The proteins were then transferred to a PVDF membrane (Bio-Rad). After blocking with PBS containing 0.1% Tween and 5% milk for 1 h, the membranes were probed with the following primary antibodies: anti-Gapdh (Cell Signaling Technology, 2118) and anti-Zeb1 (Cell Signaling Technology, 3396; the antibody was raised against a peptide with Asp846, the *Cellophane* mutation truncating the protein after Tyr902) overnight at 4 °C. Membranes were washed three times with PBS containing 0.1% Tween, and secondary antibodies were added for incubation for one hour at RT. Anti-rabbit and anti-mouse HRP conjugate secondary antibodies were provided by Jackson ImmunoResearch. Proteins were revealed with a Chemiluminescence Western Lightening Plus kit (Perkin-Elmer).

RNA-seq analysis

Thymic suspensions were stained in combination with anti-CD3, anti-CD4, anti-CD8, anti-CD69, and anti-TCRβ and subsequently sorted into different subsets using a FACSAria Cell Sorter (Becton-Dickinson, San Jose, USA). The purity of the sorted cell populations was over 98%, as measured by flow cytometry. RNA libraries were prepared as previously described.[60] Briefly, total RNA was purified from 5×10^4 sorted thymocytes using the Direct-Zol RNA microprep kit (Zymo Research) according to the manufacturer's instructions and was quantified using the QuantiFluor RNA system (Promega). One microliter of 10 μM oligo-dT primer and 1 μl of 10 mM dNTP mix were added to 0.15 ng of total RNA in a final volume of 2.3 μl. Oligo-dT cells were hybridized for 3 min at 72 °C, and reverse transcription (11 cycles) was performed. PCR preamplification was then conducted using 16 cycles. The cDNA was purified with Ampure XP beads (Beckman Coulter), and the cDNA quality was checked with D5000 screen tape and analyzed on a Tape Station 4200 (Agilent). Three nanograms of cDNA was tagmented using a NextEra XT DNA sample preparation kit (Illumina). The tagged fragments were further amplified and purified with Ampure XP beads (Beckman Coulter). The tagged library quality was checked with D1000 screen tape and analyzed

on a Tape Station 4200 (Agilent). Sequencing was performed with the GenomEast platform by a member of the "France Génomique" consortium (ANR-10-INBS- 0009) on an Illumina HiSeq 4000 sequencing instrument (read length of 1×50 nt).

Measurements of TCR signaling

Calcium response. WT and *Cellophane* thymocytes were first barcoded with anti-CD45 coupled with different fluorochromes and then stained at RT with fluorescent anti-CD4, anti-CD8, anti-CD69, anti-TCRβ, anti-CD25, and anti-CD44 antibodies, followed by staining with Indo-1 (1 µM, Life Technologies) at a concentration of 1×10^7 cells/ml for 30 min at 37 °C. Following two washes at 4 °C, the cells were resuspended in RPMI medium (0.2% BSA and 25 mM HEPES) and were incubated at 37 °C for 5–10 min prior to acquisition. The samples were acquired on an LSRII (BD) as follows: 15 s of baseline acquisition, addition of anti-CD3 biotin (2C11, 10 µg/ml), acquisition for 1 min 30 s, addition of streptavidin (Life Technologies, 10 µg/ml), and acquisition for another 3–5 min.

Phosphorylation events. Different samples corresponding to different mice were barcoded by labeling them with a series of anti-CD45 antibodies coupled with different fluorochromes. For phospho-flow staining, 3×10^6 mixed thymocytes were stained using biotinylated CD3 (2C11, 5 µg/ml) and other surface markers for 15 min, followed by streptavidin (Life Technologies, 10 µg/ml) stimulation and fixation by the addition of 10 volumes of Lyse/Fix at the indicated time points. The levels of pErk, pS6, or pAkt were normalized according to the MFI, which was detected in the nonstimulated condition (regarded as 100%) for each mouse.

In silico analyses

The functional annotations of DEGs were performed using Metascape[37] or STRING[38] using the default parameters. In addition, we used several functionalities of the ImmGen database browser[29] to generate some of the figures included in the supplementary information.

Statistical analysis

Statistical analyses were performed using Prism 5 (GraphPad Software). Two-tailed unpaired *t*-tests, paired *t*-tests, and ANOVA with Bonferroni correction were used as indicated. We used the hypergeometric test and the Benjamini–Hochberg *p* value correction algorithm to calculate if the enrichment of the overlap between the gene lists was statistically significant.

ACKNOWLEDGEMENTS

The authors acknowledge the contribution of the SFR Biosciences facilities (UMS3444/CNRS, ENSL, UCBL, and US8/INSERM), particularly the Plateau de Biologie Expérimentale de la Souris and the flow cytometry facility. We thank Bruce Beutler for sharing the *Cellophane* mutant mice. We also thank Andrew Griffiths and Kiyoto Kurima for discussions regarding *Twirler* mutant mice and Fotini Gounari and Christophe Benoist for providing RNA-seq/ChIP-seq data on T cell development. The TW lab is supported by the Agence Nationale de la Recherche (ANR *GAMBLER* to TW and ANR JC *BaNK* to AM) and the Institut National du Cancer and receives institutional grants from the Institut National de la Santé et de la Recherche Médicale (INSERM), Centre National de la Recherche Scientifique (CNRS), Université Claude Bernard Lyon and ENS de Lyon, and the Joint Research Institute for Science and Society (JORISS). JZ is the recipient of a fellowship from the China Scholarship Council (CSC). RS and YGH were funded by an FRM grant (AJE20161236686) to YGH.

AUTHOR CONTRIBUTIONS

JZ, AB, MW, DL, DEC, ALM, AR, and AM performed the experiments. RS and QM performed the in silico analyses. JC, LG, and YGH provided reagents and conceptual insight and helped write the paper. TW wrote the paper and supervised the work.

ADDITIONAL INFORMATION

The online version of this article (https://doi.org/10.1038/s41423-020-0459-y) contains supplementary material.

Competing interests: The authors declare no competing interests.

REFERENCES

1. Shah, D. K. & Zúñiga-Pflücker, J. C. An overview of the intrathymic intricacies of T cell development. *J. Immunol.* **192**, 4017–4023 (2014).
2. Rothenberg, E. V., Moore, J. E. & Yui, M. A. Launching the T-cell-lineage developmental programme. *Nat. Rev. Immunol.* **8**, 9–21 (2008).
3. Kurd, N. & Robey, E. A. T-cell selection in the thymus: a spatial and temporal perspective. *Immunol. Rev.* **271**, 114–126 (2016).
4. Hogquist, K. A. & Jameson, S. C. The self-obsession of T cells: how TCR signaling thresholds affect fate "decisions" and effector function. *Nat. Immunol.* **15**, 815–823 (2014).
5. Gascoigne, N. R. J., Rybakin, V., Acuto, O. & Brzostek, J. TCR signal strength and T cell development. *Annu. Rev. Cell Dev. Biol.* **32**, 327–348 (2016).
6. Moran, A. E. et al. T cell receptor signal strength in Treg and iNKT cell development demonstrated by a novel fluorescent reporter mouse. *J. Exp. Med.* **208**, 1279–1289 (2011).
7. Godfrey, D. I., Uldrich, A. P., McCluskey, J., Rossjohn, J. & Moody, D. B. The burgeoning family of unconventional T cells. *Nat. Immunol.* **16**, 1114–1123 (2015).
8. Kronenberg, M. & Kinjo, Y. Innate-like recognition of microbes by invariant natural killer T cells. *Curr. Opin. Immunol.* **21**, 6 (2009).
9. Tuttle, K. D. et al. TCR signal strength controls thymic differentiation of iNKT cell subsets. *Nat. Commun.* **9**, 2650 (2018).
10. Zhao, M. et al. Altered thymic differentiation and modulation of arthritis by invariant NKT cells expressing mutant ZAP70. *Nat. Commun.* **9**, 2627 (2018).
11. Malhotra, N. et al. SOX4 controls invariant NKT cell differentiation by tuning TCR signaling. *J. Exp. Med* **215**, 2887–2900 (2018).
12. Ziętara, N. et al. Critical role for miR-181a/b-1 in agonist selection of invariant natural killer T cells. *Proc. Natl Acad. Sci. USA* **110**, 7407–7412 (2013).
13. Henao-Mejia, J. et al. The microRNA miR-181 is a critical cellular metabolic rheostat essential for NKT cell ontogenesis and lymphocyte development and homeostasis. *Immunity* **38**, 984–997 (2013).
14. Wencker, M. et al. Innate-like T cells straddle innate and adaptive immunity by altering antigen-receptor responsiveness. *Nat. Immunol.* **15**, 80–87 (2014).
15. Seo, W. & Taniuchi, I. Transcriptional regulation of early T-cell development in the thymus. *Eur. J. Immunol.* **46**, 531–538 (2016).
16. Maillard, I., Fang, T. & Pear, W. S. Regulation of lymphoid development, differentiation, and function by the Notch pathway. *Annu Rev. Immunol.* **23**, 945–974 (2005).
17. Murre, C. Helix-loop-helix proteins and lymphocyte development. *Nat. Immunol.* **6**, 1079–1086 (2005).
18. Hosokawa, H. & Rothenberg, E. V. Cytokines, transcription factors, and the initiation of T-cell development. *Cold Spring Harb. Perspect. Biol.* **10**, a028621 (2018).
19. Gheldof, A., Hulpiau, P., van Roy, F., De Craene, B. & Berx, G. Evolutionary functional analysis and molecular regulation of the ZEB transcription factors. *Cell Mol. Life Sci. CMLS* **69**, 2527–2541 (2012).
20. Takagi, T., Moribe, H. & Kondoh, H. Higashi Y. DeltaEF1, a zinc finger and homeodomain transcription factor, is required for skeleton patterning in multiple lineages. *Dev. Camb. Engl.* **125**, 21–31 (1998).
21. Caramel, J., Ligier, M. & Puisieux, A. Pleiotropic roles for ZEB1 in cancer. *Cancer Res.* **78**, 30–35 (2018).
22. Conidi, A. et al. Few Smad proteins and many Smad-interacting proteins yield multiple functions and action modes in TGFβ/BMP signaling in vivo. *Cytokine Growth Factor Rev.* **22**, 287–300 (2011).
23. Scott, C. L. & Omilusik, K. D. ZEBs: novel players in immune cell development and function. *Trends Immunol.* **40**, 431–446 (2019).
24. van Helden, M. J. et al. Terminal NK cell maturation is controlled by concerted actions of T-bet and Zeb2 and is essential for melanoma rejection. *J. Exp. Med.* **212**, 2015–2025 (2015).
25. Dominguez, C. X. et al. The transcription factors ZEB2 and T-bet cooperate to program cytotoxic T cell terminal differentiation in response to LCMV viral infection. *J. Exp. Med.* **212**, 2041–2056 (2015).
26. Omilusik, K. D. et al. Transcriptional repressor ZEB2 promotes terminal differentiation of CD8+ effector and memory T cell populations during infection. *J. Exp. Med.* **212**, 2027–2039 (2015).
27. Higashi, Y. et al. Impairment of T cell development in deltaEF1 mutant mice. *J. Exp. Med.* **185**, 1467–1479 (1997).

28. Arnold, C. N. et al. A forward genetic screen reveals roles for Nfkbid, Zeb1, and Ruvbl2 in humoral immunity. *Proc. Natl Acad. Sci.* **109**, 12286–12293 (2012).
29. Heng, T. S. P. & Painter, M. W., Immunological Genome Project Consortium. The Immunological Genome Project: networks of gene expression in immune cells. *Nat. Immunol.* **9**, 1091–1094 (2008).
30. Guan, T. et al. ZEB1, ZEB2, and the miR-200 family form a counterregulatory network to regulate CD8+ T cell fates. *J. Exp. Med.* **215**, 1153–1168 (2018).
31. Jones, M. E. & Zhuang, Y. Stage-specific functions of E-proteins at the β-selection and T-cell receptor checkpoints during thymocyte development. *Immunol. Res.* **49**, 202–215 (2011).
32. Emmanuel, A. O. et al. TCF-1 and HEB cooperate to establish the epigenetic and transcription profiles of CD4+CD8+ thymocytes. *Nat. Immunol.* **19**, 1366–1378 (2018).
33. Rahim, M. M. A. et al. Ly49 receptors: innate and adaptive immune paradigms. *Front. Immunol.* **5**, 145 (2014).
34. Grigoriadou, K., Boucontet, L. & Pereira, P. Most IL-4-producing gamma delta thymocytes of adult mice originate from fetal precursors. *J. Immunol.* **171**, 2413–2420 (2003).
35. Gapin, L. iNKT cell autoreactivity: what is "self" and how is it recognized? *Nat. Rev. Immunol.* **10**, 272–277 (2010).
36. Tuttle, K. D. & Gapin, L. Characterization of thymic development of natural killer T cell subsets by multiparameter flow cytometry. *Methods Mol. Biol. Clifton NJ* **1799**, 121–133 (2018).
37. Zhou, Y. et al. Metascape provides a biologist-oriented resource for the analysis of systems-level datasets. *Nat. Commun.* **10**, 1523 (2019).
38. Szklarczyk, D. et al. STRING v10: protein-protein interaction networks, integrated over the tree of life. *Nucleic Acids Res.* **43**, D447–D452 (2015).
39. Liston, A. et al. Impairment of organ-specific T cell negative selection by diabetes susceptibility genes: genomic analysis by mRNA profiling. *Genome Biol.* **8**, R12 (2007).
40. Kastner, P. et al. Bcl11b represses a mature T-cell gene expression program in immature CD4(+)CD8(+) thymocytes. *Eur. J. Immunol.* **40**, 2143–2154 (2010).
41. Yoshida, H. et al. The cis-regulatory atlas of the mouse immune system. *Cell* **176**, 897–912.e20 (2019).
42. Bedel, R. et al. Effective functional maturation of invariant natural killer T cells is constrained by negative selection and T-cell antigen receptor affinity. *Proc. Natl Acad. Sci.* **111**, E119–E128 (2014).
43. Hayes, S. M. & Love, P. E. Strength of signal: a fundamental mechanism for cell fate specification. *Immunol. Rev.* **209**, 170–175 (2006).
44. Haks, M. C. et al. Attenuation of gammadeltaTCR signaling efficiently diverts thymocytes to the alphabeta lineage. *Immunity* **22**, 595–606 (2005).
45. Alonzo, E. S. et al. Development of promyelocytic zinc finger and ThPOK-expressing innate gamma delta T cells is controlled by strength of TCR signaling and Id3. *J. Immunol.* **184**, 1268–1279 (2010).
46. Ilangumaran, S. et al. Loss of GIMAP5 (GTPase of immunity-associated nucleotide binding protein 5) impairs calcium signaling in rat T lymphocytes. *Mol. Immunol.* **46**, 1256–1259 (2009).
47. Howie, D. et al. MS4A4B is a GITR-associated membrane adapter, expressed by regulatory T cells, which modulates T cell activation. *J. Immunol.* **183**, 4197–4204 (2009).
48. Carlson, C. M. et al. Kruppel-like factor 2 regulates thymocyte and T-cell migration. *Nature* **442**, 299–302 (2006).
49. Gubbels Bupp, M. R. et al. T cells require Foxo1 to populate the peripheral lymphoid organs. *Eur. J. Immunol.* **39**, 2991–2999 (2009).
50. Li, L. & Bhatia, R. Molecular pathways: stem cell quiescence. *Clin. Cancer Res J. Am. Assoc. Cancer Res.* **17**, 4936–4941 (2011).
51. Hedrick, S. M., Michelini, R. H., Doedens, A. L., Goldrath, A. W. & Stone, E. L. FOXO transcription factors throughout T cell biology. *Nat. Publ. Group* **12**, 649–662. (2012).
52. Shi, L. Z. et al. Gfi1-Foxo1 axis controls the fidelity of effector gene expression and developmental maturation of thymocytes. *Proc. Natl Acad. Sci. USA* **114**, E67–E74. (2017).
53. D'Cruz, L. M., Knell, J., Fujimoto, J. K. & Goldrath, A. W. An essential role for the transcription factor HEB in thymocyte survival, Tcra rearrangement and the development of natural killer T cells. *Nat. Immunol.* **11**, 240–249 (2010).
54. Brabletz, T. et al. Negative regulation of CD4 expression in T cells by the transcriptional repressor ZEB. *Int. Immunol.* **11**, 1701–1708 (1999).
55. Postigo, A. A., Ward, E., Skeath, J. B. & Dean, D. C. zfh-1, the *Drosophila* homologue of ZEB, is a transcriptional repressor that regulates somatic myogenesis. *Mol. Cell Biol.* **19**, 7255–7263 (1999).
56. Grégoire, J. M. & Roméo, P. H. T-cell expression of the human GATA-3 gene is regulated by a non-lineage-specific silencer. *J. Biol. Chem.* **274**, 6567–6578 (1999).
57. Wang, L. et al. Genomic profiling of Sézary syndrome identifies alterations of key T cell signaling and differentiation genes. *Nat. Genet.* **47**, 1426–1434 (2015).
58. Mishra, A. et al. Mechanism, consequences, and therapeutic targeting of abnormal IL15 signaling in cutaneous T-cell lymphoma. *Cancer Discov.* **6**, 986–1005 (2016).
59. Doisne, J.-M. et al. iNKT cell development is orchestrated by different branches of TGF- signaling. *J. Exp. Med.* **206**, 1365–1378 (2009).
60. Picelli, S. et al. Full-length RNA-seq from single cells using Smart-seq2. *Nat. Protoc.* **9**, 171–181 (2014).